NADH–Ubiquinone Oxidoreductases of the *Escherichia coli* Aerobic Respiratory Chain

Kazunobu Matsushita,[‡,§] Tomoko Ohnishi,[∥] and H. Ronald Kaback*[,§]

Roche Institute of Molecular Biology, Roche Research Center, Nutley, New Jersey 07110, and Department of Biochemistry and Biophysics, University of Pennsylvania, Philadelphia, Pennsylvania 19104

Received April 20, 1987; Revised Manuscript Received June 29, 1987

ABSTRACT: Deamino-NADH/ubiquinone 1 oxidoreductase activity in membrane preparations from *Escherichia coli* GR19N is 20–50% of NADH/ubiquinone 1 oxidoreductase activity. In comparison, membranes from *E. coli* IY91, which contain amplified levels of NADH dehydrogenase, exhibit about 100-fold higher NADH/ubiquinone 1 reductase activity but about 20-fold less deamino-NADH/ubiquinone 1 reductase activity. Deamino-NADH/ubiquinone 1 reductase is more sensitive than NADH/ubiquinone 1 reductase activity to inhibition by 3-undecyl-2-hydroxy-1,4-naphthoquinone, piericidin A, or myxothiazol. Furthermore, GR19N membranes exhibit two apparent K_ms for NADH but only one for deamino-NADH. Inside-out membrane vesicles from *E. coli* GR19N generate a H^+ electrochemical gradient (interior positive and acid) during electron transfer from deamino-NADH to ubiquinone 1 that is large and stable relative to that observed with NADH as substrate. Generation of the H^+ electrochemical gradient in the presence of deamino-NADH is inhibited by 3-undecyl-2-hydroxy-1,4-naphthoquinone and is not observed in IY91 membrane vesicles or in vesicles from GR19N that are deficient in deamino-NADH/ubiquinone 1 reductase activity. The data provide a strong indication that the *E. coli* aerobic respiratory chain contains two species of NADH dehydrogenases: (i) an enzyme (NADH dh I) that reacts with deamino-NADH or NADH whose turnover leads to generation of a H^+ electrochemical gradient at a site between the primary dehydrogenase and ubiquinone and (ii) an enzyme (NADH dh II) that reacts with NADH exclusively whose turnover does not lead to generation of a H^+ electrochemical gradient between the primary dehydrogenase and ubiquinone 1.

The nature of the membrane-bound dehydrogenases that utilize NADH as substrate and their role in the generation of the H^+ electrochemical gradient ($\Delta\bar{\mu}_{H^+}$)[1] in *Escherichia coli* are unresolved. Transport studies with right-side-out membrane vesicles from *E. coli* ML308-225 led initially to the suggestion that NADH oxidation is not energy-conserving (Barnes & Kaback, 1971; Ramos et al., 1976), while studies with inside-out (ISO) vesicles (cf. Reenstra et al., 1980) suggest strongly that NADH oxidation is coupled to the generation of $\Delta\bar{\mu}_{H^+}$. Furthermore, on the basis of observations with intact cells demonstrating that oxidation of malate or endogenous substrates produces higher H^+/O ratios than oxidation of succinate or lactate, Pool and Haddock (1975) postulated that there is an "energy-coupling site" in the NADH dehydrogenase region of the respiratory chain. In contrast, Brookman et al. (1979) concluded that there is no proton translocation associated with the NADH dehydrogenase segment of the *E. coli* respiratory chain, on the basis of the observation that proton translocation associated with NADH/menadione reductase activity is diminised by an *unc* mutation.

By using immunoadsorption and quantitative crossed immunoelectrophoresis, Owen and Kaback (1978, 1979b) demonstrated that membrane vesicles prepared from *E. coli* by osmotic lysis retain essentially the same polarity and configuration as the cytoplasmic membrane in the intact cell. It was also demonstrated (Owen & Kaback, 1979a) that the membrane contains at least two immunologically distinct NADH dehydrogenases, both on the cytoplasmic surface. One of the NADH dehydrogenases (antigen 15) contains non-heme iron (Owen et al., 1980a) and can be distinguished from the other NADH dehydrogenase (antigen 19/27) by its ability to react with reduced nicotinamide hypoxanthine dinucleotide (deamino-NADH or d-NADH) (Owen et al., 1980b). Independently, Ingledew et al. (1980) provided evidence for iron–sulfur clusters with low E_m values in the NADH dehydrogenase region of the *E. coli* respiratory chain. Finally, a gene encoding one of the NADH dehydrogenases (*ndh*) was cloned and sequenced (Young et al., 1978, 1981), and the enzyme was purified from membranes of a strain harboring a multicopy recombinant plasmid (Jaworowski et al., 1981a). Purified enzyme consists of a single polypeptide containing flavin adenine dinucleotide (FAD), but no iron, and is highly active with ubiquinone 1 (Q_1) as electron acceptor (Jaworowski et al., 1981a,b). The purified enzyme is also able to reconstitute cyanide-sensitive NADH oxidase activity in membranes from an NADH dehydrogenase deficient mutant (Jaworowski et al., 1981b). These data presented by Young and associates suggest that there is no iron–sulfur cluster and no energy-coupling site associated with this dehydrogenase.

Recently, $\Delta\bar{\mu}_{H^+}$ generation in ISO vesicles from *E. coli* GR19N, which contain cyanide-sensitive cytochrome *o* as the sole terminal oxidase, was compared by using D-lactate, Q_1H_2, or NADH as electron donors (Matsushita & Kaback, 1986).

* Author to whom correspondence should be addressed.

[‡] Present address: Department of Agricultural Chemistry, Faculty of Agriculture, Yamaguchi University, Yamaguchi 753, Japan.

[§] Roche Institute of Molecular Biology.

[∥] University of Pennyslvania.

[1] Abbreviations: $\Delta\bar{\mu}_{H^+}$, H^+ electrochemical gradient; ISO, inside out; d-NADH, reduced nicotinamide hypoxanthine dinucleotide; FAD, flavin adenine dinucleotide; Q_1, ubiquinone 1; UHNQ, 3-undecyl-2-hydroxy-1,4-naphthoquinone; diBA-C_2-(5), bis(1,3-diethylbarbituric acid) pentamethine oxonol; KP_i, potassium phosphate; DTT, dithiothreitol; DCIP, dichlorophenolindophenol; $\Delta\Psi$, membrane potential; Hepes, 4-(2-hydroxyethyl)-1-piperazineethanesulfonic acid.

0006-2960/87/0426-7732$01.50/0

The experiments demonstrate clearly that NADH oxidation leads to generation of a significantly greater $\Delta\bar{\mu}_{H^+}$ (interior positive and acid) and that electron flow from NADH to Q_1, but not from D-lactate to Q_1, generates $\Delta\bar{\mu}_{H^+}$ in the presence of cyanide. It was concluded, therefore, that the region of the respiratory chain between NADH dehydrogenase and Q_8, the physiological quinone in aerobic *E. coli*, conserves respiratory energy in the form of $\Delta\bar{\mu}_{H^+}$.

The data presented here confirm and extend previous data (Owen & Kaback, 1979b; Matsushita & Kaback, 1986) by demonstrating that membranes from *E. coli* GR19N contain two distinct NADH dehydrogenases with different biochemical properties. The enzymes are characterized kinetically in terms of substrate specificity and inhibitor sensitivity and with regard to their ability to generate $\Delta\bar{\mu}_{H^+}$ in the region of the respiratory chain between the primary dehydrogenases and Q_8. One of the dehydrogenases (termed NADH dh I) utilizes both d-NADH and NADH, and its turnover generates $\Delta\bar{\mu}_{H^+}$ in the presence of cyanide and Q_1. The other dehydrogenase (termed NADH dh II) utilizes NADH exclusively, and electron flow between the enzyme and Q_8 does not lead to generation of $\Delta\bar{\mu}_{H^+}$.

Experimental Procedures

Materials

NADH, d-NADH, sodium cholate, and DNase I were purchased from Sigma. 3-Undecyl-2-hydroxy-1,4-naphthoquinone (UHNQ) was purchased from Aldrich Chemical Co. and myxothiazol from Boehringer. Bis(1,3-diethylbarbituric acid) pentamethine oxonol [diBA-C_2-(5)] was generously donated by Dr. Alan Waggoner, piericidin A by Drs. N. Takahashi and C. I. Ragan, and Q_1 by Hoffmann-La Roche Inc. All other chemicals were of reagent grade and obtained from commercial sources.

Methods

Bacterial Strains. E. coli GR19N (*cyd*$^-$) (Green & Gennis, 1983) was grown aerobically into late logarithmic phase in minimal medium containing sodium lactate and casamino acids as described (Matsushita et al., 1983). *E. coli* IY91, which harbors a recombinant plasmid encoding *ndh* (Jaworowski et al., 1981b), was kindly supplied by Dr. I. G. Young and was grown aerobically into late logarithmic phase in minimal medium containing mannitol as sole carbon source (Campbell & Young, 1983).

Preparation of Membrane Vesicles. Cells were harvested by centrifugation and washed once in 50 mM potassium phosphate (KP_i; pH 7.5). Washed cells were resuspended in 50 mM KP_i (pH 7.5) containing 5 mM $MgSO_4$ (4 mL/g wet weight of cells), and DNase was added to a concentration of 10 μg/mL. For preparation of ISO vesicles, cell suspensions were passed through a French pressure cell at low shear forces (5000 psi) (Reenstra et al., 1980; Matsushita & Kaback, 1986); to prepare membranes for enzymatic assays, high shear forces were used (16000 psi). Unbroken cells and cell debris were removed by centrifugation at 10000*g* for 10 min, and the supernatant was centrifuged at 120000*g* for 2 h in order to sediment the membrane fraction. The pellet contained two clearly demarcated portions, a lower transparent layer and an upper red layer. The loose, red layer was resuspended in 50 mM KP_i (pH 7.5)/5 mM $MgSO_4$ at half the volume of the initial suspension and centrifuged at 120000*g* for 2 h. As indicated, dithiothreitol (DTT) and glycerol were added to final concentrations of 1 mM and 10%, respectively.

Enzyme Assays. Each oxidoreductase activity of the NADH oxidase system was measured at 25 °C spectrophotometrically. Reaction mixtures contained membranes, 2.5 mM potassium cyanide, and a given electron acceptor in 1 mL of 50 mM KP_i (pH 7.5)/5 mM $MgSO_4$. Reactions were started by addition of 125 μM NADH or d-NADH as indicated. Q_1 reductase activity was measured at 340 nm with 80 μM Q_1, dichlorophenolindophenol (DCIP) reductase at 600 nm with 50 μM DCIP, and ferricyanide reductase at 420 nm with 1 mM ferricyanide; activity was calculated by using millimolar extinction coefficients of 6.81, 16.5, and 1.0, respectively, for Q_1, DCIP, and ferricyanide. NADH oxidase activity was also measured spectrophotometrically by following absorbance at 340 nm. Reactions were performed in the same manner, except for the addition of potassium cyanide and a given electron acceptor, and activity was calculated by using a millimolar extinction coefficient of 6.22. Other Q_1 reductase activities were measured by following reduction of Q_1 at 275 nm. Reactions were performed under the same conditions as those described for NADH/Q_1 reductase, except that substrates were added at final concentrations of 10 mM, and activity was calculated with an extinction coefficient of 12.25 mM^{-1}.

Determination of Membrane Potential ($\Delta\Psi$). Generation of $\Delta\Psi$ (interior positive) in ISO vesicles was monitored by following fluorescence quenching of diBA-C_2-(5) (Waggoner, 1979; Matsushita & Kaback, 1986). Reaction mixtures (2 mL, total volume) contained 50 mM KP_i (pH 7.5), 5 mM $MgSO_4$, 2 μM diBA-C_2-(5), and ISO vesicles (0.2–0.4 mg of protein) with or without 2.5 mM potassium cyanide. Experiments were carried out at 25 °C, and fluorescence emission was measured at 614 nm with excitation at 588 nm.

Protein Assays. Protein was determined with amido black (Schaffner & Weissmann, 1973) or by a modification of the Lowry method (Dulley & Grieve, 1975).

Results

E. coli GR19N Membranes Contain Two Distinct NADH Dehydrogenases. As shown by Owen et al. (1980b), *E. coli* ML308-225 membranes contain two components that oxidize NADH: one (antigen 19/27), which oxidizes NADH exclusively, does not contain iron and exhibits immunological identity with dihydrolipoyl dehydrogenase and a second (antigen 15), which oxidizes d-NADH in addition to NADH, contains iron. Initial attempts to extend these observations to membranes from *E. coli* GR19N, which has a more simple respiratory chain (Matsushita & Kaback, 1986), demonstrate that d-NADH oxidation in these membranes is unstable relative to NADH oxidation (Table I). Thus, in membranes prepared without extensive washing and/or prolonged incubation, d-NADH and NADH oxidase activities are relatively high, and activity toward d-NADH is about 50% of that observed with NADH (the value varies from 20 to 50% from one preparation to another). After washing 3 times, however, d-NADH oxidase and d-NADH/Q_1 reductase activities are severely diminished, while NADH oxidase and NADH/Q_1 reductase exhibit higher specific activities. Interestingly, d-NADH/ferricyanide and d-NADH/DCIP reductase activities, like the corresponding activities with NADH as electron donor, are relatively unaffected, suggesting that extensive washing inactivates a component that reacts specifically with Q_1. In contrast, membranes prepared from *E. coli* IY91, which contain amplified levels of NADH dehydrogenase, exhibit about 100-fold greater NADH/Q_1 reductase and significantly higher levels of NADH oxidase, NADH/ferricyanide reductase, and NADH/DCIP reductase activities but markedly diminished corresponding activities toward d-NADH. The data are clearly consistent with the idea that

Table I: Enzyme Activities (μmol Oxidized min^{-1} mg^{-1}) of the NADH Oxidase System in Membranes from *E. coli* GR19N and IY91[a]

enzyme	GR19N NADH	GR19N d-NADH	GR19N washed NADH	GR19N washed d-NADH	IY91 NADH	IY91 d-NADH
oxidase	0.91	0.44	1.63	0.04	12.1	0.04
Q_1 reductase	0.94	0.41	1.48	0.08	64.0	0.02
ferricyanide reductase	1.87	1.42	1.56	0.50	17.6	0.24
DCIP reductase	0.35	0.21	0.66	0.20	7.0	0.03

[a] Membranes from *E. coli* GR19N or IY91 were prepared as described under Methods, and washed membranes from GR19N were prepared by washing the membranes 3 times in 50 mM Hepes (pH 7.5) containing 0.1 M KCl and 5 mM $MgSO_4$. Each enzyme activity was measured as described under Methods.

Table II: K_m Values for NADH or d-NADH in *E. coli* GR19N Membranes[a]

assay	K_m for NADH (μM)	K_m for d-NADH (μM)
oxidase	5.3–6.6, 48	5.0–7.9
Q_1 reductase	14.7, 50	9.7[b]
	52[c]	50[d]

[a] K_m values were calculated from Lineweaver–Burk plots as shown in Figure 1. Each enzyme activity was measured as described under Methods. NADH or d-NADH was used at concentrations ranging from 17 to 200 μM. [b] The reaction was started by addition of d-NADH. [c] The reaction was done in the presence of 100 nmol of UHNQ/mg of protein. [d] The reaction was started by addition of Q_1.

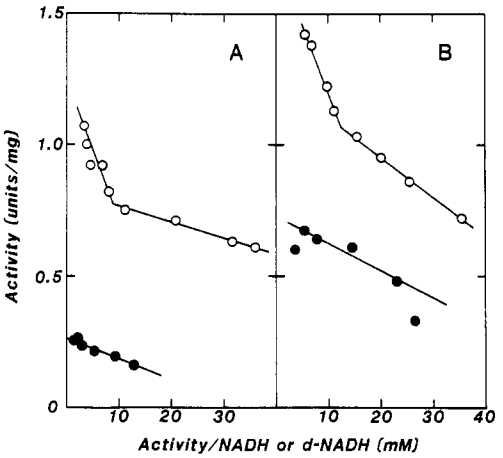

FIGURE 1: Kinetics of NADH oxidase system in membranes from *E. coli* GR19N. (A) NADH oxidase (○) and d-NADH oxidase (●) activities were measured with different concentrations of NADH or d-NADH as described under Methods. (B) NADH/Q_1 reductase (○) and d-NADH/Q_1 reductase (●) activities were measured by starting the reactions with different concentrations of NADH or d-NADH.

GR19N membranes contain two species of NADH dehydrogenases, one of which utilizes either NADH or d-NADH as substrate (NADH dh I) and another that utilizes NADH exclusively (NADH dh II).

GR19N membranes exhibit two apparent K_ms for NADH (Figure 1), the values of which are 5–15 μM and about 50 μM with oxygen or Q_1 as electron acceptor (Table II). However, in the same membranes, only a single apparent K_m of 5–10 μM is observed for d-NADH when the reaction is initiated by addition of substrate (Figure 1 and Table II). Parenthetically, it is noteworthy that d-NADH/Q_1 reductase activity is decreased by about half and the apparent K_m increases to about 50 μM when the membranes are incubated with d-NADH in the absence of electron acceptor (Table II).

Since NADH dh I and II presumably donate electrons to Q, the two enzymes might be expected to exhibit differential sensitivities to quinone analogues when tested for NADH/Q_1 reductase activity. As shown in Figure 2, d-NADH/Q_1 reductase activity is more sensitive to UHNO than NADH/Q_1 reductase, exhibiting 50% inhibition at about 50–70 nmol/mg

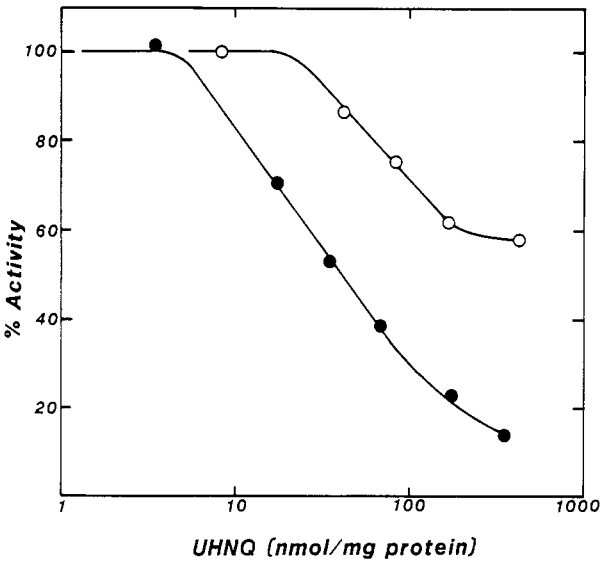

FIGURE 2: UHNQ inhibition of NADH/Q_1 reductase and d-NADH/Q_1 reductase activities in membranes from *E. coli* GR19N. Each enzyme activity was measured as described under Methods, following preincubation of membranes with given concentrations of UHNQ for 2–3 min. (○) NADH/Q_1 reductase; (●) d-NADH/Q_1 reductase.

Table III: Inhibition of NADH/Q_1 Reductase and d-NADH/Q_1 Reductase Activities by Quinone Analogues[a]

inhibitor	inhibition (%) GR19N membranes NADH	GR19N membranes d-NADH	IY91 membranes, NADH
UHNQ	30.0	75.2	−2.0
		12.8[b]	
		22.4[c]	
piericidin A	33.4	80.4	
myxothiazol	11.0	56.4	0.7[d]

[a] Q_1 reductase activity was measured as described under Methods after the membranes were preincubated with 100 nmol/mg of membrane protein of each inhibitor for 2–3 min. [b] The value shows the percent inhibition of d-NADH/ferricyanide reductase activity with UHNQ. [c] Percent inhibition of d-NADH/DCIP reductase activity with UHNQ. [d] Percent inhibition with 500 nmol/mg of membrane protein of myxothiazol.

of protein. In the same range of UHNQ concentrations, NADH/Q_1 reductase activity is inhibited to a marginal extent. Piericidin A and myxothiazol also inhibit d-NADH/Q_1 reductase activity significantly with lesser effects on NADH/Q_1 reductase and, importantly, neither UHNQ nor myxothiazol significantly inhibits NADH/Q_1 reductase in IY91 membranes (Table III). Finally, UHNQ causes only slight inhibition of d-NADH/ferricyanide or d-NADH/DCIP reductase activities, suggesting that electron flow to these acceptors is not mediated by Q.

$\Delta\bar{\mu}_{H^+}$ Generation in the NADH/Q_1 Region of the Respiratory Chain. A study of fluorescence quenching of diBA-C_2-(5), a voltage-sensitive probe that responds to $\Delta\Psi$ (interior

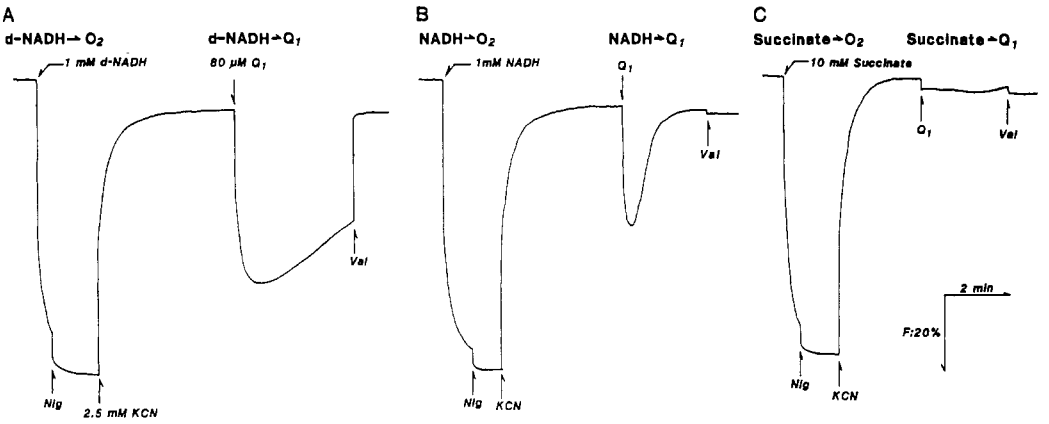

FIGURE 3: $\Delta\Psi$ generation during electron transfer from d-NADH (A), NADH (B), or succinate (C) to oxygen or Q_1 in ISO vesicles from *E. coli* GR19N. Fluorescence quenching of diBA-C_2-(5) was monitored as described under Methods with 0.25 mg of ISO vesicle protein. Reactions were initiated by addition of the indicated substrate, followed by successive addition of 0.025 μM nigericin (Nig), KCN, Q_1, and 1 μM valinomycin (Val).

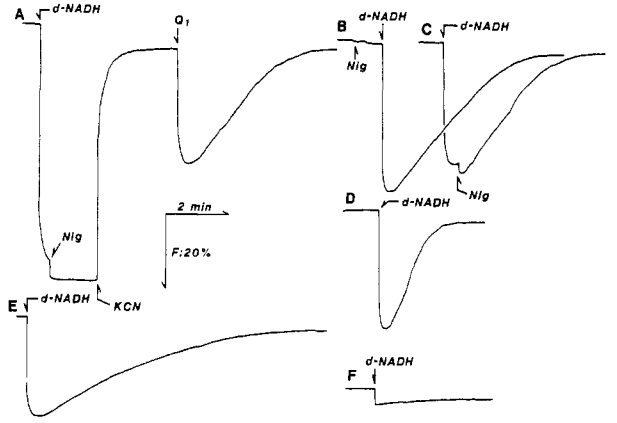

FIGURE 4: $\Delta\Psi$ generation during electron transfer from d-NADH to Q_1 in ISO vesicles from *E. coli* GR19N. Fluorescence quenching of diBA-C_2-(5) was followed as described in Figure 3. Reaction A was performed by using 0.25 mg of membrane protein and by successive addition of 1 mM d-NADH, 0.025 μM nigericin (Nig), 2.5 mM KCN, and 80 μM Q_1, as indicated. Reactions B and C were initiated by d-NADH after addition of Nig (B) or before addition of Nig (C) to assay mixtures containing 0.25 mg of membrane protein, 80 μM Q_1, and 2.5 mM KCN. Reaction D was carried out as described for reaction B except that 40 μM Q_1 was used instead of 80 μM. Reaction E was carried out with 0.125 mg of membrane protein as described for reaction B, and reaction F was also performed as described for reaction B, but 10 μM UHNQ was also present in the reaction mixtures.

positive) demonstrated (Matsushita & Kaback, 1986) that electron flow from NADH to either Q_1 or ferricyanide generates $\Delta\bar{\mu}_{H^+}$ in ISO vesicles from *E. coli* GR19N. However, the magnitude of the $\Delta\bar{\mu}_{H^+}$ generated is relatively small and transient. Since it is now apparent that the membranes contain two species of NADH dh, similar studies were performed in order to study comparative $\Delta\bar{\mu}_{H^+}$ generation with NADH, d-NADH, or other substrates (Figure 3). Electron transfer from d-NADH to Q_1 clearly generates a $\Delta\Psi$ (interior positive) that is larger and more stable than that observed during electron transfer from NADH to Q_1 (compare parts A and B of Figure 3), while electron transfer from succinate, D-lactate, or L-lactate to Q_1 generates no significant $\Delta\bar{\mu}_{H^+}$ (Figure 3C and Table IV). Fluorescence quenching due to electron flow from d-NADH to Q_1 is reversed by valinomycin, which dissipates $\Delta\Psi$ (Figure 3A), and enhanced by nigericin, which collapses the pH gradient with an increase in $\Delta\Psi$ (parts B and C of Figure 4). Furthermore, fluorescence quenching induced by d-NADH and Q_1 in the presence of cyanide is dependent on the amount of membrane protein added to the reaction

Table IV: Activity and $\Delta\Psi$ Generation of Q_1 Reductases in *E. coli* ISO Vesicles[a]

Q_1 reductase	enzyme activity (μmol of Q_1 reduced min^{-1} mg^{-1})	diBA-C_2-(5) quenching ($\Delta F/F$, %)
NADH/Q_1	1.25	34.8
d-NADH/Q_1	0.44	52.7
L-lactate/Q_1	1.95	0
D-lactate/Q_1	0.40	0
succinate/Q_1	0.27	0

[a] Enzyme assays and diBA-C_2-(5) quenching were performed in the presence of 2.5 mM KCN as described under Methods.

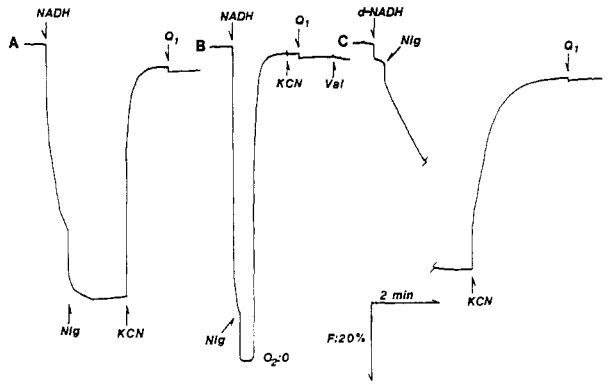

FIGURE 5: $\Delta\Psi$ generation in ISO vesicles deficient in NADH dh I activity. Fluorescence quenching of diBA-C_2-(5) was measured as described in Figures 3 and 4. (A) Reaction mixtures contained 0.205 mg of protein from GR19N membrane vesicles washed extensively as described in Table I, and the reaction was carried out by successive addition of 1 mM NADH, 0.025 μM Nig, 2.5 mM KCN, and 80 μM Q_1. (B) Reaction mixtures contained 0.134 mg of IY91 membrane protein. Reactions were initiated with 1 mM NADH, and 1 μM Val was added at the end of the reaction. (C) Reaction mixtures contained 0.268 mg of IY91 membrane protein, and the reactions were initiated with 1 mM d-NADH.

mixtures and on the concentration of Q_1, and the phenomenon is blocked by UHNQ (parts D–F of Figure 4). Finally, the magnitude of the quench is greater when the reactions are initiated with d-NADH rather than Q_1 (compare parts A and B of Figure 4), an observation similar to that described above for d-NADH/Q_1 reductase activity.

When d-NADH dh I in GR19N membranes is inactivated by prolonged washing, $\Delta\bar{\mu}_{H^+}$ is generated during electron flow from NADH to oxygen because of the activity of cytochrome *o* (Matsushita & Kaback, 1986). However, no significant $\Delta\bar{\mu}_{H^+}$ is generated during electron flow from NADH to Q_1 (Figure 5A). Similarly, ISO vesicles from IY91 generate

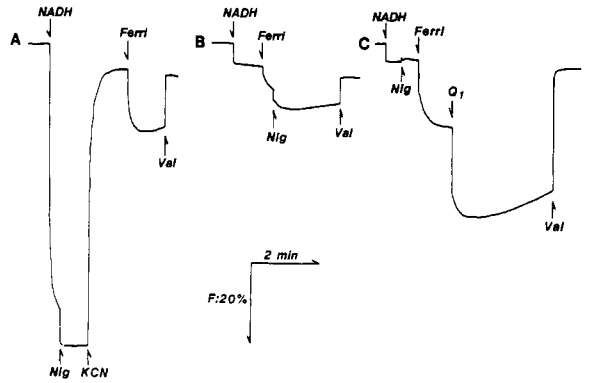

FIGURE 6: $\Delta\Psi$ generation during electron flow from NADH to ferricyanide in *E. coli* GR19N ISO vesicles. Fluorescence quenching of diBA-C_2-(5) was measured as described in Figures 3 and 4 by using 0.25 mg of GR19N membrane protein. (A) Reactions were initiated with 1 mM NADH, followed by successive addition of 0.025 μM Nig, 2.5 mM KCN, 1 mM potassium ferricyanide (Ferri), and 1 μM Val. (B and C) Reactions were performed in the presence of 2.5 mM KCN as described in (A).

$\Delta\bar{\mu}_{H^+}$ in the presence of NADH and oxygen, but not in the presence of NADH and cyanide with Q_1 as electron acceptor (Figure 5B). Although IY91 vesicles retain some d-NADH/Q_1 reductase activity, no $\Delta\bar{\mu}_{H^+}$ generation is observed during electron flow from d-NADH to Q_1 (Figure 5C).

Electron flow from NADH or d-NADH to ferricyanide also leads to fluorescence quenching of diBA-C_2-(5) in ISO vesicles from GR19N, but the effect is significantly smaller than that observed with Q_1 (parts A and B of Figure 6). Interestingly, addition of both Q_1 and ferricyanide causes a greater degree of fluorescence quenching than addition of either electron acceptor independently (Figure 6C). This effect can be rationalized by the ability of ferricyanide to regenerate Q_1 from Q_1H_2 chemically.

Discussion

The data presented here confirm and extend earlier indications (Owen & Kaback, 1979b; Owen et al., 1980b) that there are two distinct species of NADH dehydrogenases in the membrane of *E. coli*. One of these enzymes, NADH dh I, reacts with d-NADH as well as NADH, while the other, NADH dh II, reacts exclusively with NADH. NADH dh I is unstable and is inactivated by repeated washing of the membranes. Furthermore, NADH dh I seems to be inactivated by preincubation with d-NADH in the absence of electron acceptors as noted initially by Gutman et al. (1968) and by Owen et al. (1980b). NADH dh I and II can also be distinguished on the basis of apparent affinity for d-NADH; NADH dh I exhibits a lower apparent K_m for the electron donor than NADH dh II. In addition, the two dehydrogenases probably have different specificities for electron acceptors; Q_1 appears to be a more favorable acceptor for NADH dh II, while ferricyanide functions better with NADH dh I (cf. Tables I and IV). From the properties described, it seems highly likely that NADH dh II in *E. coli* GR19N is the same enzyme as that encoded by the *ndh* gene which was cloned and sequenced by Young et al. (1978, 1981). The product of *ndh* is a single polypeptide with a molecular weight of 47 304 and high Q_1 reductase activity that contains FAD but no iron (Jaworowski et al., 1981a,b). In contrast, NADH dh I has properties similar to those of the enzyme described by Gutman et al. (1968) and by Owen et al. (1980b) that has not been purified. Although data are not shown, NADH dh I and II can be separated by cholate extraction, but thus far NADH dh I has not been solubilized in an active state.

Another difference between NADH dh I and II is differential sensitivity to quinone analogues. NADH/Q_1 reductase activity catalyzed by NADH dh I is significantly more sensitive to inhibition by UHNQ, piericidin A, and myxothiazol. It is interesting that each of these quinone analogues is a potent inhibitor of complex I or III in the mitochondrial respiratory chain. Thus, although NADH dh I and II both react with Q_1, it is possible that only NADH dh I reduces the physiological ubiquinone, Q_8, in the membrane in the same manner as mitochondrial complexes I and III.

It seems likely that NADH dh I, but not NADH dh II, is able to generate $\Delta\bar{\mu}_{H^+}$ during electron flow between the primary dehydrogenase and Q. ISO vesicles from GR19N, which contain cytochrome *o* as sole terminal oxidase, can generate $\Delta\bar{\mu}_{H^+}$ during electron flow from either NADH dh I or NADH dh II to oxygen due to turnover of cytochrome *o* (Matsushita et al., 1983, 1984). However, when electron transfer from the primary dehydrogenases to Q is examined by studying fluorescence quenching of diBA-C_2-(5) in the presence of cyanide and Q_1, it is apparent that turnover of NADH dh I only is coupled to generation of $\Delta\bar{\mu}_{H^+}$. This conclusion is also consistent with the following observations: (i) Under the conditions described, electron flow from d-NADH to Q_1 does not lead to generation of $\Delta\bar{\mu}_{H^+}$ in membranes from IY91 or in washed membranes from GR19N, neither of which contains active NADH dh I. (ii) UHNQ, a potent inhibitor of NADH dh I, blocks $\Delta\bar{\mu}_{H^+}$ generation during electron flow from d-NADH to Q_1.

Finally, the observations as a whole may explain why NADH/Q_1 reductase activity gives rise to a small, transient $\Delta\bar{\mu}_{H^+}$ relative to that given by d-NADH/Q_1 reductase. Electron flow from NADH to Q_1 is catalyzed by both NADH dh I and II, both dehydrogenases utilize NADH, and Q_1 accepts electrons preferentially from NADH dh II in a mechanism that does not lead to $\Delta\bar{\mu}_{H^+}$ generation. Therefore, when NADH is used as electron donor, Q_1 is consumed rapidly, and much of the overall reaction is unproductive in terms of $\Delta\bar{\mu}_{H^+}$ generation. Furthermore, when ferricyanide is added with Q_1, a larger, more stable $\Delta\bar{\mu}_{H^+}$ is observed (cf. Figure 6C) because ferricyanide regenerates Q_1 chemically from Q_1H_2. In contrast, electron flow from d-NADH to Q_1 is catalyzed by NADH dh I exclusively, Q_1 is consumed relatively slowly, and the $\Delta\bar{\mu}_{H^+}$ generated is of greater mangitude and more long-lived.

Acknowledgments

A portion of this work was performed in the Laboratory of Applied Microbiology, Department of Agricultural Chemistry, Faculty of Agriculture, Yamaguchi University, Yamaguchi, Japan, and we are indebted to Professor M. Ameyama for encouragement and support.

Registry No. NADH, 58-68-4; d-NADH, 22052-73-9; UHNQ, 41245-59-4; piericidin A, 2738-64-9; myxothiazol, 76706-55-3; NADH–ubiquinone reductase, 9028-04-0.

References

Barnes, E. M., & Kaback, H. R. (1971) *J. Biol. Chem. 246*, 5518.

Brookman, J. J., Downie, J. A., Gibson, F., Cox, G. B., & Rosenberg, H. (1979) *J. Bacteriol. 137*, 705.

Crowe, B. A., Owen, P., Patil, D. S., & Cammack, R. (1983) *Eur. J. Biochem. 137*, 191.

Dulley, J. R., & Grieve, P. A. (1975) *Anal. Biochem. 64*, 136.

Green, G. N., & Gennis, R. B. (1983) *J. Bacteriol. 154*, 1269.

Gutman, M., Schejter, A., & Avi-Dor, Y. (1968) *Biochim. Biophys. Acta 162*, 506.

Ingledew, W. J., Reid, G. A., Poole, R. K., Blum, H., & Ohnishi, T. (1980) *FEBS Lett. 111*, 223.
Jaworowski, A., Campbell, H. D., Poulis, M. I., & Young, I. G. (1981a) *Biochemistry 20*, 2041.
Jaworowski, A., Mayo, G., Shae, D. C., Campbell, H. D., & Young, I. G. (1981b) *Biochemistry 20*, 3621.
Matsushita, K., & Kaback, H. R. (1986) *Biochemistry 25*, 2321.
Matsushita, K., Patel, L., Gennis, R. B., & Kaback, H. R. (1983) *Proc. Natl. Acad. Sci. U.S.A. 80*, 4889.
Matsushita, K., Patel, L., & Kaback, H. R. (1984) *Biochemistry 23*, 4703.
Murakami, H., Kita, K., Oya, H., & Anraku, Y. (1985) *FEMS Microbiol. Lett. 30*, 307.
Owen, P., & Kaback, H. R. (1978) *Proc. Natl. Acad. Sci. U.S.A. 75*, 3148.
Owen, P., & Kaback, H. R. (1979a) *Biochemistry 18*, 1413.
Owen, P., & Kaback, H. R. (1979b) *Biochemistry 18*, 1422.
Owen, P., Kaczorowski, G. J., & Kaback, H. R. (1980a) *Biochemistry 19*, 596.
Owen, P., Kaback, H. R., & Graeme-Cook, K. A. (1980b) *FEMS Microbiol. Lett. 7*, 345.
Poole, R. K., & Haddock, B. A. (1975) *Biochem. J. 152*, 537.
Ramos, S., Schuldiner, S., & Kaback, H. R. (1976) *Proc. Natl. Acad. Sci. U.S.A. 73*, 1892.
Reenstra, W. W., Patel, L., Rottenberg, H., & Kaback, H. R. (1980) *Biochemistry 19*, 1.
Schaffner, W., & Weissman, C. (1973) *Anal. Biochem. 56*, 502.
Waggoner, A. (1979) *Annu. Rev. Biophys. Bioeng. 8*, 47.
Young, I. G., Jaworowski, A., & Poulis, M. I. (1978) *Gene 4*, 25.
Young, I. G., Rogers, B. L., Campbell, H. D., Jaworowski, A., & Shaw, D. C. (1981) *Eur. J. Biochem. 116*, 165.

Raman Spectroscopy of Interferon-Induced 2′,5′-Linked Oligoadenylates†

Joseph C. White, Robert W. Williams, and Margaret I. Johnston*
Department of Biochemistry, The Uniformed Services University of the Health Sciences, Bethesda, Maryland 20814-4799
Received March 23, 1987; Revised Manuscript Received June 2, 1987

ABSTRACT: Raman spectra of model compounds and of 2′,5′-oligoadenylates in D_2O were utilized to assign the Raman bands of 2′,5′-oligoadenylates. The Raman spectra of A2′pA2′pA, pA2′pA2′pA, and pppA2′pA2′pA contained features that were similar to those of adenosine, adenosine 5′-monophosphate (AMP), and adenosine 5′-triphosphate, respectively. When AMP and pA2′pA2′pA were titrated from pH 2 to 9, the normalized Raman intensity of their ionized (980 cm^{-1}) and protonated (1080 cm^{-1}) phosphate bands revealed similar pK_a's for the 5′-monophosphates. The Raman spectrum of pA2′pA2′pA was altered slightly by elevations in temperature, but not in a manner supporting the postulate that 2–5A possesses intermolecular base stacking. Major differences in the Raman spectrum of 2′,5′- and 3′,5′-oligoadenylates were observed in the 600–1200-cm^{-1} portion of the spectrum that arises predominately from ribose and phosphate vibrational modes. Phosphodiester backbone modes in A3′pA3′pA and pA3′pA3′pA produced a broad band at 802 cm^{-1} with a shoulder at 820 cm^{-1}, whereas all 2′,5′-oligoadenylates contained a major phosphodiester band at 823 cm^{-1} with a shoulder at 802 cm^{-1}. The backbone mode of pppA2′pA2′pA contained the sharpest band at 823 cm^{-1}, suggesting that the phosphodiester backbone may be more restrained in the biologically active, 5′-triphosphorylated molecule. The Raman band assignments for 2′,5′-oligoadenylates provide a foundation for using Raman spectroscopy to explore the mechanism of binding of 2′,5′-oligoadenylates to proteins.

Interferons are recognized as important biological mediators that have numerous effects on the immune system, including inhibition of viral replication. Interferons induce at least two double-stranded RNA-dependent proteins, 2′,5′-oligoadenylate synthetase and protein P_1 kinase [reviewed by Johnston and Torrence (1984)]. 2′,5′-Oligoadenylate synthetase polymerizes ATP[1] into pppA(2′pA)$_n$, where $n \geq 2$ (2–5A). 2′,5′-Oligoadenylates activate a latent endoribonuclease (RNase L) that degrades RNA and contributes to the translational inhibition caused by double-stranded RNA (dsRNA) (Kerr & Brown, 1978; Kerr et al., 1974; Lebleu et al., 1976; Sen et al., 1976).

The unique nature of these 2′,5′-oligoadenylates has prompted investigation into the structural requirements for

† This work was supported in part by The Uniformed Services University of the Health Sciences (Grant T07146 to J.C.W. and Grant GM 7159 to M.I.J.) and the National Science Foundation (Grant PCM-8443154 to R.W.W.). The opinions or assertions contained herein are the private ones of the authors and are not to be construed as official or reflecting the views of the U.S. Department of Defense or The Uniformed Services University of the Health Sciences.
* Author to whom correspondence should be addressed.

[1] Abbreviations: 2–5A (trimer triphosphate), 5′-*O*-triphosphoryladenylyl(2′,5′)adenylyl(2′,5′)adenosine [pppA2′p(A2′p)$_n$A, where n is usually 1–3]; pA2′pA2′pA (trimer monophosphate), 5′-*O*-monophosphoryladenylyl(2′,5′)adenylyl(2′,5′)adenosine; pA2′pA3′pA, 5′-*O*-monophosphoryladenylyl(2′,5′)adenylyl(3′,5′)adenosine; pA3′pA2′pA, 5′-*O*-monophosphoryladenylyl(3′,5′)adenylyl(2′,5′)adenosine; A2′pA2′pA (trimer core), adenylyl(2′,5′)adenylyl(2′,5′)adenosine; A3′pA3′pA, adenylyl(3′,5′)adenylyl(3′,5′)adenosine; pA2′pA^{8Br}2′pA^{8Br}, 5′-*O*-monophosphoryladenylyl(2′,5′)-8-bromoadenylyl-8-bromoadenosine; dsRNA, double-stranded RNA; RNase L, 2–5A-dependent endoribonuclease; HEPES, 4-(2-hydroxyethyl)-1-piperazineethanesulfonic acid; AMP, adenosine 5′-monophosphate; ADP, adenosine 5′-diphosphate; ATP, adenosine 5′-triphosphate; HPLC, high-performance liquid chromatography; CD, circular dichroism; NMR, nuclear magnetic resonance.